Controlling Optomechanical Libration with the Degree of Polarization

J. A. Zielińska,[1,*] F. van der Laan,[1] A. Norrman,[1,2] M. Rimlinger,[1] R. Reimann,[1,3] L. Novotny,[1] and M. Frimmer[1]
[1]Photonics Laboratory, ETH Zürich, CH-8093 Zürich, Switzerland
[2]Center for Photonics Sciences, University of Eastern Finland, P.O. Box 111, FI-80101 Joensuu, Finland
[3]Quantum Research Center, Technology Innovation Institute, Abu Dhabi, United Arab Emirates

(Received 11 January 2023; revised 7 March 2023; accepted 4 April 2023; published 16 May 2023)

Control of the potential energy and free evolution lie at the heart of levitodynamics as key requirements for sensing, wave function expansion, and mechanical squeezing protocols. Here, we experimentally demonstrate versatile control over the optical potential governing the libration motion of a levitated anisotropic nanoparticle. This control is achieved by introducing the degree of polarization as a new tool for rotational levitodynamics. We demonstrate thermally driven free rotation of a levitated anisotropic scatterer around its short axis and we use the rotational degrees of freedom to probe the local spin of a strongly focused laser beam.

DOI: 10.1103/PhysRevLett.130.203603

Introduction.—Levitodynamics is the science of controlling the motion of levitated mesoscopic objects [1]. The field has received growing attention in the last decade as a platform for force, torque, and electric field sensing [2]. Next to the translational degrees of freedom, the rotational dynamics of levitated anisotropic nanoparticles (which are similar to molecular orientation dynamics [3]) offer particularly promising opportunities. More specifically, new functionalities demonstrated for optically levitated rotors include controllable diffusion [4], gyroscopic stabilization [5], spinning with GHz rotation rates [6–9], and the realization of rotational "washboard potentials" by carefully trading off conservative and nonconservative torques in elliptically polarized fields [4,10].

A particularly enticing prospect is to harness levitated rotors as torque sensors [8], in applications ranging from photonic torque microscopy [11–16], to seismology [17,18] and space-based alignment procedures [19]. Another use case are tests of quantum coherence at macroscopic scales [20,21]. Significant progress has been made on cooling libration motion using parametric [22] and linear feedback cooling [23], as well as via coupling to a cavity [24,25]. Once the ground state is achieved, control over the depth and inversion of the potential may enable the generation of large delocalized orientational states [26,27] and the preparation of mechanical squeezed states [28].

Therefore, to realize the full promise of levitated rotors, a scheme is required to release a librator from the optical potential pinning its orientation, allowing it to freely evolve. In this state, the system becomes an optically suspended gyroscope that is extremely sensitive to dc torques, in full analogy to previously developed dc force sensing schemes [29]. The open question is how to deactivate the optical potential used to trap the levitated object's orientation while keeping the trapping potential for its center-of-mass (c.m.) motion fully intact.

In this Letter we demonstrate control over the conservative libration potential of an optically levitated particle. Our scheme makes use of the degree of polarization of the trapping field. We experimentally realize near-zero libration frequencies up to the point where the libration potential is too shallow to trap the orientation, giving way to thermally driven Brownian motion of the levitated rotor. Additionally, for particles with cylindrical symmetry (dumbbells), we observe the signature of the transverse spin of light locally present in a strongly focused trapping beam.

Key concept.—Consider an anisotropic dipolar point scatterer of polarizability $\boldsymbol{\alpha} = \mathrm{diag}(\alpha_1, \alpha_2, \alpha_3)$ in the body frame (spanned by unit vectors $\mathbf{e}_1$, $\mathbf{e}_2$, $\mathbf{e}_3$), with $\alpha_3 > \alpha_2 > \alpha_1$, as illustrated in Fig. 1. The orientation of the particle with respect to the lab frame is described by the three Euler angles Φ, Θ, and Ψ (see Supplemental Material [30]). In a field linearly polarized along x in the lab frame, the particle will align with its axis of largest polarizability $\mathbf{e}_3$ to the polarization axis x ($\Phi = \Theta = 0$), while it can freely rotate by any angle Ψ around its long axis $\mathbf{e}_3$. Small deviations of the long axis $\mathbf{e}_3$ from the polarization axis

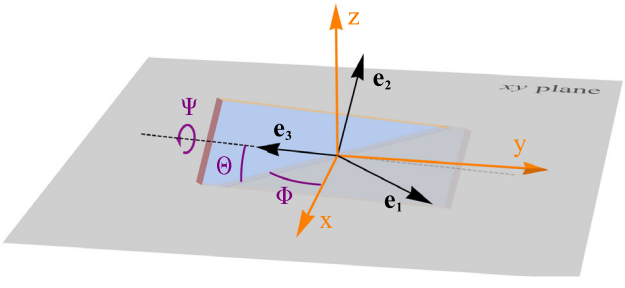

FIG. 1. The orientation of an anisotropic particle's body frame (given by $\mathbf{e}_1$, $\mathbf{e}_2$, $\mathbf{e}_3$) relative to the lab frame (x, y, z) is described by the three angles Φ, Θ, and Ψ.

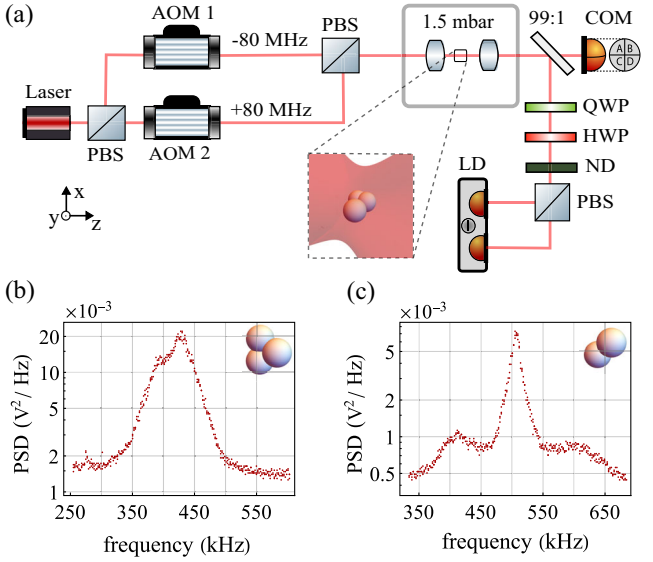

FIG. 2. (a) Simplified schematic of the experimental setup. The two polarization components of a laser beam are separated and each frequency shifted by ±80 MHz, respectively, with an acousto-optic modulator (AOM). The components' amplitudes E_x and E_y are varied by adjusting the driving powers of the AOMs. After recombining the polarization components on a polarizing beam splitter (PBS), the beam is focused in a vacuum chamber with a high-NA lens to form an optical trap with variable degree of polarization. The libration signal is detected in the forward direction using a combination of a quarter-wave plate (QWP), half-wave plate (HWP), a neutral density filter (ND), a PBS, and a balanced detector (LD). (b) Power spectral density (PSD) of a particle cluster in a linearly polarized trap. (c) PSD of a dumbbell in a linearly polarized trap.

represent libration modes, i.e., harmonic oscillator degrees of freedom, described by the angles Φ and Θ.

Let us now consider an unpolarized electric field, whose field vector remains in the xy plane. Here, the particle will "lie flat" in the polarization plane, i.e., align with its axis of smallest polarizability $\mathbf{e}_1$ along the z axis. Deviations from this alignment, i.e., tilts out of the polarization plane, again represent two libration modes described by the angles Θ and Ψ. At the same time, the particle can freely rotate by any angle Φ, as the field vector has no preferred direction in the xy plane. Accordingly, both in a linearly and in an unpolarized field, one angular degree of freedom is free. Importantly, in the unpolarized case, the free rotation is measurable by available detection schemes [22,38] and therefore highly attractive for torque sensing applications. In the following, we experimentally investigate the dynamics of a levitated rotor as it is transitioned from a linearly polarized to an unpolarized trapping field.

Experiment.—At the heart of our experimental setup, illustrated in Fig. 2(a), is an optical trap with variable degree of polarization (DOP), formed by focusing a trapping beam with a lens (NA = 0.8) inside a vacuum chamber (pressure 1.5 mbar). To vary the DOP, a laser beam (wavelength 1550 nm) is split into two components with orthogonal linear polarization, which are then frequency shifted with acousto-optic modulators (AOMs) by ±80 MHz, respectively. The frequency-shifted polarization components are subsequently recombined on a polarizing beam splitter to form the trapping beam (power 450 mW), which propagates along the z direction. Spherical silica nanoparticles (nominal diameter 143 nm) are loaded into the trap with a nebulizer. The dynamics of the trapped object is detected using forward-scattered light. The c.m. motion is recorded using a quadrant photodiode, and the libration signal using a standard homodyne detection scheme [22].

In this Letter, we focus on two distinct classes of anisotropic particles, identified by their characteristic libration spectra shown in Figs. 2(b) and 2(c). The first class are "clusters," that is, objects composed of more than two particles, described by a fully anisotropic polarizability tensor (as the particle symbolically depicted in Fig. 1). The cluster spectrum shown in Fig. 2(b) exhibits two modes at 390 and 425 kHz, respectively, which we associate with the libration modes described by the angles Θ and Φ from Fig. 1. The second class of anisotropic particles are dumbbells (cylindrically symmetric objects composed of two spherical particles in touching contact), characterized by a sharp libration peak flanked by broad shoulders, as shown in Fig. 2(c). This spectrum originates from two libration modes that are coupled by the thermally driven spinning around the symmetry axis [22,23,39].

Degree of polarization.—Having introduced the spectra for linearly polarized light we now turn to fields of variable DOP. In our setup, the tweezer field before the trapping lens reads $\mathbf{E} = (E_x e^{i\omega_x t}, E_y e^{i\omega_y t}, 0)^T$, where the angular frequency difference $\Delta\omega = \omega_x - \omega_y = 2\pi \times 160$ MHz is kept constant, while the real-valued amplitudes E_x and E_y can be controlled with the AOMs (see Supplemental Material for details [30]). The instantaneous polarization state of the trapping beam (before focusing) is described via the four Stokes parameters [40].

$$S_0 = E_x^2 + E_y^2, \tag{1a}$$

$$S_1 = E_x^2 - E_y^2, \tag{1b}$$

$$S_2 = 2E_x E_y \cos(\Delta\omega t), \tag{1c}$$

$$S_3 = -2E_x E_y \sin(\Delta\omega t). \tag{1d}$$

The DOP is defined as

$$\mathcal{P} = \sqrt{\langle S_1\rangle^2 + \langle S_2\rangle^2 + \langle S_3\rangle^2}/\langle S_0\rangle, \tag{2}$$

where $\langle\cdot\rangle$ denotes the time average [41]. Since the optical modulation frequency $\Delta\omega$ is more than 2 orders of magnitude larger than the libration dynamics, the cosine

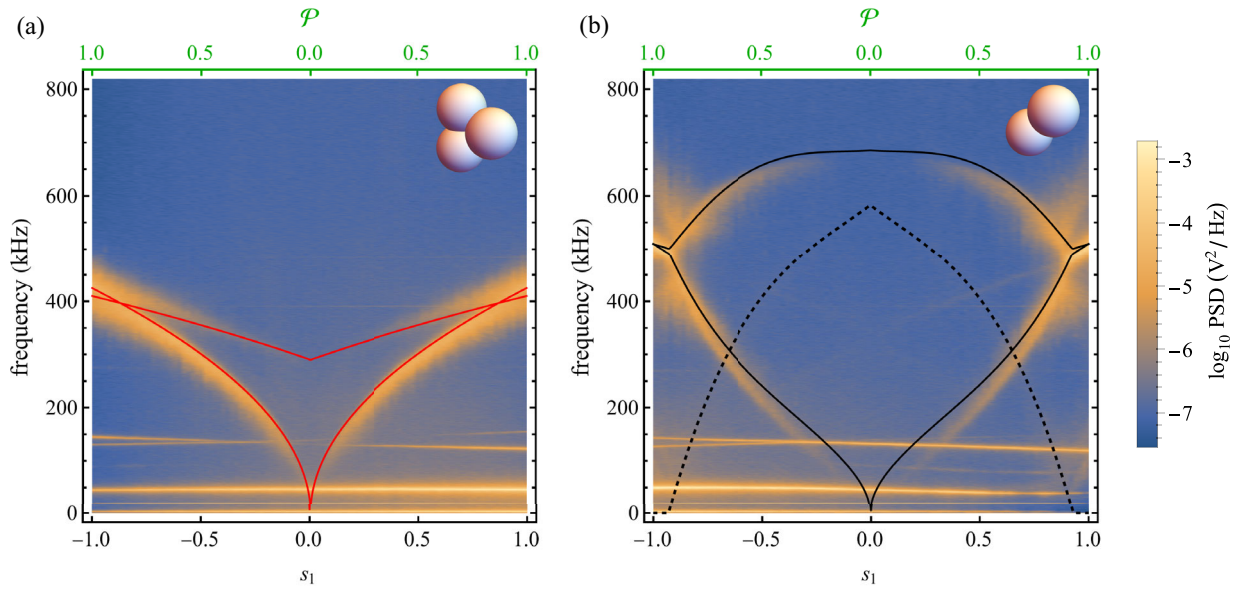

FIG. 3. PSDs measured by the libration detector as a function of the DOP and the normalized Stokes parameter s_1 of the trapping beam. Each subfigure consists of 100 PSDs, where the first one ($s_1 = -1$) corresponds to y polarized trapping light and the last one ($s_1 = 1$) to x polarized trapping light. In the case of $s_1 = 0$ the trapping beam is effectively unpolarized and the frequency corresponding to libration in the xy plane tends to zero. Frequencies corresponding to translational c.m. motion are visible as horizontal lines in the range between 40 and 150 kHz. (a) Cluster (nonrotationally symmetric particle). Red lines show theoretical prediction calculated from Eqs. (3a) and (3b) using only libration frequencies measured at the linear polarization setting. (b) Dumbbell (cylindrically symmetric particle). Black solid lines are precession frequencies calculated from the theoretical model including spinning of the dumbbell along its long axis [30], with $\omega_s/2\pi$ (proportional to the spinning rate) shown as a dashed black line.

and the sine terms average out and the DOP simplifies to $\mathcal{P} = |s_1|$, where $s_1 = S_1/S_0$. The upper bound, $\mathcal{P} = 1$, corresponds to fully linearly polarized light, while the lower bound, $\mathcal{P} = 0$, denotes unpolarized light. The intermediate regime, $0 < \mathcal{P} < 1$, describes partial polarization.

Results.—Let us discuss our experimental observations for a cluster trapped in a beam with variable DOP. In Fig. 3(a), we show in false color the power spectral density (PSD) of the libration signal as a function of frequency and $\mathcal{P}$. For linearly polarized trapping light ($\mathcal{P} = 1$), we observe the spectrum from Fig. 2(b), with a feature composed of two closely spaced peaks near 400 kHz. As the DOP is reduced ($\mathcal{P} < 1$), the two peaks split and their frequencies decrease. Remarkably, for unpolarized light ($\mathcal{P} = 0$) the frequency of one of the modes vanishes, while the frequency of the second mode approaches 300 kHz.

Our experimental observations for a trapped dumbbell, shown in Fig. 3(b), strikingly differ from that of a cluster. The single peak at 500 kHz (surrounded by broad shoulders) observed in linearly polarized light ($\mathcal{P} = 1$), see Fig. 2(c), splits in two as the DOP is reduced ($\mathcal{P} < 1$). In contrast to the cluster, the dumbbell exhibits one mode that shifts to higher frequencies and settles at 680 kHz for unpolarized light ($\mathcal{P} = 0$), while the second mode frequency tends towards zero, where its signal strength vanishes.

Model.—To understand our observations, we model the orientational dynamics of an anisotropic dipolar scatterer in a field of variable DOP. Let the scatterer be characterized by its polarizability $\boldsymbol{\alpha} = \mathrm{diag}(\alpha_1, \alpha_2, \alpha_3)$ and its tensor of inertia $\mathbf{I} = \mathrm{diag}(I_1, I_2, I_3)$, which are both diagonal in the intrinsic body frame spanned by $\mathbf{e}_1$, $\mathbf{e}_2$, $\mathbf{e}_3$. We furthermore assume $\alpha_1 \le \alpha_2 \le \alpha_3$ and $I_1 \ge I_2 \ge I_3$. We calculate the potential energy of a fully anisotropic scatterer in a field of variable DOP as a function of the orientation angles Φ, Θ, and Ψ and identify the global energy minimum (see Supplemental Material [30]). Small deviations of the orientation angles Φ, Θ, and Ψ from their equilibrium values resemble, to first order, harmonic oscillator degrees of freedom, whose characteristic libration frequencies are given by

$$\Omega_1 = A_1\sqrt{\mathcal{P}}, \tag{3a}$$

$$\Omega_2 = A_2\sqrt{\frac{1+\mathcal{P}}{2}}, \tag{3b}$$

$$\Omega_3 = A_3\sqrt{\frac{1-\mathcal{P}}{2}}, \tag{3c}$$

respectively, where $A_i = [(|\alpha_j - \alpha_k|S_0)/2I_i]^{1/2}$ and $\{i, j, k\}$ are permutations of $\{1, 2, 3\}$.

Equations (3a)–(3c) indicate that we can directly control the libration potential governing the orientation of the rotor via the DOP. Although our detection is only sensitive to

libration in the xy plane [38], the coupling between the different libration modes [39] is responsible for the second libration mode in the spectrum. Since our detection scheme is not sensitive to the third libration mode, the frequency Ω_3 is not visible in the libration spectra. To compare our theoretical prediction with our measurement, we plot the calculated values for the libration frequencies Ω_1 and Ω_2 from Eqs. (3a) and (3b) as red lines in the measurement of the trapped cluster in Fig. 3(a). The required parameters A_1 and A_2 are defined by the libration frequencies extracted at $\mathcal{P} = 1$. The theoretical lines trace the observed libration frequencies remarkably well, demonstrating that our model correctly captures the rotational dynamics and providing strong support for our initial assumption that the trapped object is a cluster without symmetry. In a field with $\mathcal{P} < 0.05$, the cluster's libration frequency Ω_1 vanishes as the libration potential is not deep enough to trap the angle Φ at room temperature. In other words, the orientation angle Φ undergoes thermally driven Brownian motion.

Let us turn our attention to the dynamics of the trapped dumbbells. Inspection of Eq. (3c) shows that for an object of cylindrical symmetry A_3 and therefore also Ω_3 vanish. This observation intuitively makes sense, since such a scatterer can always freely rotate around its long axis. However, for dumbbells, the libration frequencies as a function of $\mathcal{P}$, experimentally observed in Fig. 3(b), deviate significantly from those predicted by Eqs. (3a) and (3b). As has been pointed out before [23,39], the spinning of the dumbbell at a stationary rate $\dot{\Psi}_0$ around its axis of symmetry couples the libration modes with frequencies Ω_1 and Ω_2 into precession modes with frequencies Ω_A and Ω_B according to

$$(\Omega_A - \Omega_B)^2 = \omega_s^2 + (\Omega_1 - \Omega_2)^2, \tag{4}$$

with the coupling rate $\omega_s = \mu\dot{\Psi}_0$ and the inertial coupling constant $\mu = (I_1 - I_3)/I_1$. We interpret the salient libration features in our data in Fig. 3(b) as the precession frequencies Ω_A and Ω_B of the dumbbell, and fit their functional dependence with Eq. (4), where Ω_1 and Ω_2 are in turn given by Eqs. (3a) and (3b). The fit [black solid lines in Fig. 3(b)] describes our experimental observation very well and yields a fitted coupling rate ω_s, shown as the dashed black line in Fig. 3(b) [30]. We conclude that the rate of spinning around the long axis in our experiment reaches $\dot{\Psi}_0 = 2\pi \times 200$ kHz in the regime of unpolarized light $\mathcal{P} = 0$, where we used the dumbbell's length-to-diameter ratio of $L/D \approx 1.8$ [4] to estimate the inertial coupling factor as $\mu \approx 0.375$. The actual value of $\dot{\Psi}_0$ depends on the friction coefficient [42] and the applied torque. We will explain the origin of the torque driving this spinning motion in the next section.

Discussion.—Our results in Fig. 3 demonstrate that the DOP of the trapping field allows us to control the libration frequencies of the optically levitated particle. We stress the fact that for a cluster in a field with vanishing DOP, the libration frequency Ω_1 vanishes. In other words, the cluster becomes a free rotor regarding its orientation angle around the optical z axis, while its two axes of largest moment of inertia (I_2 and I_3) are harmonically trapped in the xy plane of polarization. The situation is analogous for the dumbbell, whose long axis is harmonically trapped with characteristic frequency Ω_B in the focal xy plane in unpolarized light, while the orientation of the long axis undergoes free evolution within this plane. Thus, the DOP allows us, for the first time, to tune the angular motion of a levitated object from libration at several hundred kHz all the way to thermally driven Brownian motion. This demonstration is the main result of this Letter. We discuss the limitations of this scheme in [30].

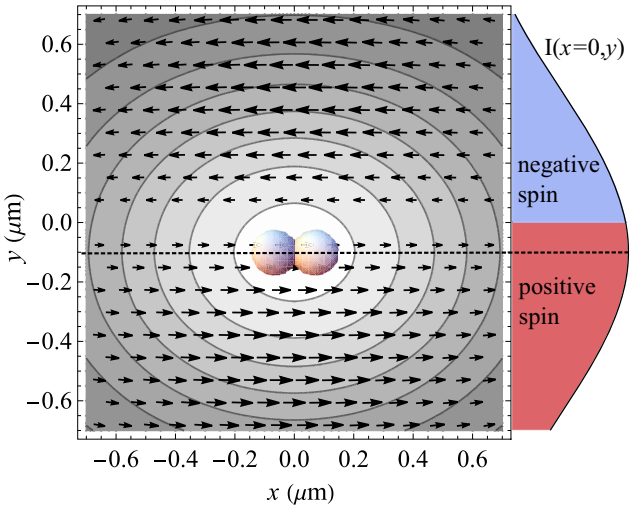

FIG. 4. Illustration of the spatial mismatch between the trapping beam components leading to a dumbbell being trapped in a region of nonzero transverse spin. A vector plot shows the transverse spin pattern in the xy plane generated by a y polarized strongly focused Gaussian beam [46]. Simultaneously, we show the dumbbell (to scale) trapped in the intensity maximum of an x polarized Gaussian beam (contour plot) of higher power, displaced by 100 nm from $y = 0$. On the right we plot the intensity profile $I(x = 0, y)$, indicating regions with spin pointing in the negative and positive x direction.

Let us now provide an explanation for the torque that drives the trapped dumbbell into spinning motion around its long axis. We note that this torque must lie in the focal plane (which is the plane the dumbbell's long axis is pinned to). Strongly focused fields can indeed carry transverse spin angular momentum [43,44], which gives rise to a torque when transferred to a particle. In Fig. 4, we illustrate the transverse part of the spin vector [45] in the focal plane of a strongly focused y polarized Gaussian beam. The spin is depicted as arrows whose direction (length) indicates the spin's orientation (magnitude). The spin points predominantly along the positive (negative) x direction in the range $y < 0$ ($y > 0$). To understand how a dumbbell can be exposed to the transverse spin, we consider a trap composed of two polarization components. The optical power

of the x component is higher than that of the y component. Therefore, the x polarized component (whose intensity is illustrated as a color plot in Fig. 4) determines the position of the particle's c.m. and aligns the particle's long axis along the x direction. If we displace the x polarized beam along the y direction then the transverse spin of the y polarized beam will spin the dumbbell along its long axis, as experimentally observed. Even though the torque along the dumbbell's long axis is very weak, the effect is visible since the dumbbell is free to rotate along its long axis. We can compare the maximum value of $\omega_s/2\pi$ [reaching 600 kHz, see Fig. 3(b)] to the shoulders flanking the libration peak for $\mathcal{P} = 1$ due to thermal spinning [which are approximately 200 kHz apart, see Fig. 2(c)]. From this we conclude that the maximum torque driving the spinning motion exceeds the average absolute value of the fluctuating thermal torque by approximately a factor of 3.

We can thus explain the observed spinning motion of the dumbbell as a signature of the transverse spin angular momentum of light in a strongly focused field, together with an inevitably imperfect alignment between the two cross-polarized beams forming our trap with tunable DOP. Effectively the trapped dumbbell locally senses the spin of an additional light field. Note that, in contrast to dumbbells, clusters are not driven into rotation along their long axis by a weak transverse spin of light, since $A_3 \neq 0$ and the angle of rotation around the long axis is restrained for $\mathcal{P} < 1$ [see Eq. (3c)].

Conclusions.—We have demonstrated the complete tunability of the libration frequencies of optically levitated clusters of silica nanoparticles. This tunability is accomplished by the DOP and is independent of the c.m. trapping potential. Our Letter is important for the development of high-performance nanoscale gyroscopes and for the study of macroscopic rotational quantum physics [24,47]. Furthermore, we have found that symmetric levitated rotors respond to optical torques not only perpendicular, but also parallel to their long axis. This feature may allow addressing open questions on gas friction for rotating bodies [42] and holds promise to enable the full characterization of three-dimensional Stokes parameters [11,48–50].

The authors would like to thank A. Militaru, O. Romero-Isart, C. Gonzalez-Ballestero, and all trappers in the Photonics Laboratory for fruitful discussions. This research was supported by the European Union's Horizon 2020 research and innovation programme under Grant Agreement No. [863132] (IQLev), as well as ETH Grant No. ETH-47 20-2. A. N. thanks the Jane and Aatos Erkko Foundation (Finland) for funding.

*jzielinska@ethz.ch

[1] C. Gonzalez-Ballestero, M. Aspelmeyer, L. Novotny, R. Quidant, and O. Romero-Isart, Levitodynamics: Levitation and control of microscopic objects in vacuum, Science **374**, 3027 (2021).
[2] M. Rademacher, J. Millen, and Y. L. Li, Quantum sensing with nanoparticles for gravimetry: When bigger is better, Adv. Opt. Technol. **9**, 227 (2020).
[3] M. Lemeshko, R. V. Krems, J. M. Doyle, and S. Kais, Manipulation of molecules with electromagnetic fields, Mol. Phys. **111**, 1648 (2013).
[4] L. Bellando, M. Kleine, Y. Amarouchene, M. Perrin, and Y. Louyer, Giant diffusion of Nanomechanical Rotors in a Tilted Washboard Potential, Phys. Rev. Lett. **129**, 023602 (2022).
[5] S. Kuhn, B. A. Stickler, A. Kosloff, F. Patolsky, K. Hornberger, M. Arndt, and J. Millen, Optically driven ultra-stable nanomechanical rotor, Nat. Commun. **8**, 1670 (2017).
[6] R. Reimann, M. Doderer, E. Hebestreit, R. Diehl, M. Frimmer, D. Windey, F. Tebbenjohanns, and L. Novotny, GHz Rotation of an Optically Trapped Nanoparticle in Vacuum, Phys. Rev. Lett. **121**, 033602 (2018).
[7] J. Ahn, Z. Xu, J. Bang, Y.-H. Deng, T. M. Hoang, Q. Han, R.-M. Ma, and T. Li, Optically Levitated Nanodumbbell Torsion Balance and GHz Nanomechanical Rotor, Phys. Rev. Lett. **121**, 033603 (2018).
[8] J. Ahn, Z. Xu, J. Bang, P. Ju, X. Gao, and T. Li, Ultrasensitive torque detection with an optically levitated nanorotor, Nat. Nanotechnol. **15**, 89 (2020).
[9] F. van der Laan, R. Reimann, A. Militaru, F. Tebbenjohanns, D. Windey, M. Frimmer, and L. Novotny, Optically levitated rotor at its thermal limit of frequency stability, Phys. Rev. A **102**, 013505 (2020).
[10] S. Kuhn, A. Kosloff, B. A. Stickler, F. Patolsky, K. Hornberger, M. Arndt, and J. Millen, Full rotational control of levitated silicon nanorods, Optica **4**, 356 (2017).
[11] A. Irrera, A. Magazzù, P. Artoni, S. H. Simpson, S. Hanna, P. H. Jones, F. Priolo, P. G. Gucciardi, and O. M. Maragò, Photonic torque microscopy of the nonconservative force field for optically trapped silicon nanowires, Nano Lett. **16**, 4181 (2016).
[12] V. Svak, O. Brzobohatý, M. Šiler, P. Jákl, J. Kaňka, P. Zemánek, and S. H. Simpson, Transverse spin forces and non-equilibrium particle dynamics in a circularly polarized vacuum optical trap, Nat. Commun. **9**, 5453 (2018).
[13] Y. Arita, S. H. Simpson, P. Zemánek, and K. Dholakia, Coherent oscillations of a levitated birefringent microsphere in vacuum driven by nonconservative rotationtranslation coupling, Sci. Adv. **6**, eaaz9858 (2020).
[14] Y. Liang, S. Yan, Z. Wang, B. Yao, and M. Lei, Off-axis optical levitation and transverse spinning of metallic microparticles, Photonics Res. **9**, 2144 (2021).
[15] Y. Arita, S. H. Simpson, G. D. Bruce, E. M. Wright, P. Zemánek, and K. Dholakia, Cooling the optical-spin driven limit cycle oscillations of a levitated gyroscope, arXiv:2204.06925.
[16] Y. Hu, J. J. Kingsley-Smith, M. Nikkhou, J. A. Sabin, F. J. Rodríguez-Fortuño, X. Xu, and J. Millen, Structured transverse orbital angular momentum probed by a levitated optomechanical sensor, arXiv:2209.09759.
[17] F. Guattari, E. de Toldi, R. F. Garcia, and D. Mimoun, International Conference on Space Optics—ICSO 2018, in International Conference on Space Optics—ICSO 2018,

International Society for Optics and Photonics (SPIE, 2019), Vol. 11180, p. 1118080, 10.1117/12.2536207.

[18] J. Wassermann, T. Braun, M. Ripepe, F. Bernauer, F. Guattari, and H. Igel, The use of 6DOF measurement in volcano seismology—a first application to stromboli volcano, J. Volcanol. Geotherm. Res. **424**, 107499 (2022).

[19] J. Jin, T. Zhang, L. Kong, and K. Ma, In-orbit performance evaluation of a spaceborne high precision fiber optic gyroscope, Sensors **18**, 106 (2018).

[20] B. A. Stickler, B. Papendell, S. Kuhn, B. Schrinski, J. Millen, M. Arndt, and K. Hornberger, Probing macroscopic quantum superpositions with nanorotors, New J. Phys. **20**, 122001 (2018).

[21] B. Schrinski, B. A. Stickler, and K. Hornberger, Interferometric control of nanorotor alignment, Phys. Rev. A **105**, L021502 (2022).

[22] F. van der Laan, F. Tebbenjohanns, R. Reimann, J. Vijayan, L. Novotny, and M. Frimmer, Sub-Kelvin Feedback Cooling and Heating Dynamics of an Optically Levitated Librator, Phys. Rev. Lett. **127**, 123605 (2021).

[23] J. Bang, T. Seberson, P. Ju, J. Ahn, Z. Xu, X. Gao, F. Robicheaux, and T. Li, Five-dimensional cooling and nonlinear dynamics of an optically levitated nanodumbbell, Phys. Rev. Res. **2**, 043054 (2020).

[24] J. Schäfer, H. Rudolph, K. Hornberger, and B. A. Stickler, Cooling Nanorotors by Elliptic Coherent Scattering, Phys. Rev. Lett. **126**, 163603 (2021).

[25] A. Pontin, H. Fu, M. Toroš, T. S. Monteiro, and P. F. Barker, Simultaneous cooling of all six degrees of freedom of an optically levitated nanoparticle by elliptic coherent scattering, arXiv:2205.10193.

[26] T. Weiss, M. Roda-Llordes, E. Torrontegui, M. Aspelmeyer, and O. Romero-Isart, Large Quantum Delocalization of a Levitated Nanoparticle using Optimal Control: Applications for Force Sensing and Entangling Via Weak Forces, Phys. Rev. Lett. **127**, 023601 (2021).

[27] Once the ground state is reached, we estimate that coherent spatial expansion by a factor of 10^2 is possible even in the presence of backaction-induced heating rates reported in [22].

[28] J. Janszky and P. Adam, Strong squeezing by repeated frequency jumps, Phys. Rev. A **46**, 6091 (1992).

[29] E. Hebestreit, M. Frimmer, R. Reimann, and L. Novotny, Sensing of Static Forces with Free-Falling Nanoparticles, Phys. Rev. Lett. **121**, 063602 (2018).

[30] See Supplemental Material at http://link.aps.org/supplemental/10.1103/PhysRevLett.130.203603 for the detailed description of the experimental setup, derivation of Eqs. (3) and further discussion of spinning along the long axis driven by the transverse spin, which includes Refs. [31–37].

[31] E. W. Weisstein, From MathWorld–A Wolfram Web Resource, https://mathworld.wolfram.com/EulerAngles.html.

[32] L. D. Landau and E. M. Lifshitz, *Mechanics, Third Edition: Volume 1 (Course of Theoretical Physics)*, 3rd ed. (Butterworth-Heinemann, London, 1976).

[33] S. Rahav, I. Gilary, and S. Fishman, Effective Hamiltonians for periodically driven systems, Phys. Rev. A **68**, 013820 (2003).

[34] R. Kitamura, L. Pilon, and M. Jonasz, Optical constants of silica glass from extreme ultraviolet to far infrared at near room temperature, Appl. Opt. **46**, 8118 (2007).

[35] F. Monteiro, S. Ghosh, E. C. van Assendelft, and D. C. Moore, Optical rotation of levitated spheres in high vacuum, Phys. Rev. A **97**, 051802(R) (2018).

[36] G. M. Hale and M. R. Querry, Optical constants of water in the 200-nm to 200-μm wavelength region, Appl. Opt. **12**, 555 (1973).

[37] M. Kamba, R. Shimizu, and K. Aikawa, Nanoscale feedback control of six degrees of freedom of a near-sphere, arXiv:2303.02831.

[38] F. Tebbenjohanns, A. Militaru, A. Norrman, F. van der Laan, L. Novotny, and M. Frimmer, Optimal orientation detection of an anisotropic dipolar scatterer, Phys. Rev. A **105**, 053504 (2022).

[39] T. Seberson and F. Robicheaux, Parametric feedback cooling of rigid body nanodumbbells in levitated optomechanics, Phys. Rev. A **99**, 013821 (2019).

[40] J. J. Gil and R. Ossikovski, *Polarized Light and the Mueller Matrix Approach*, 2nd ed. (CRC Press, Boca Raton, 2022), 10.1201/9780367815578.

[41] A. Shevchenko, M. Roussey, A. T. Friberg, and T. Setälä, Polarization time of unpolarized light, Optica **4**, 64 (2017).

[42] L. Martinetz, K. Hornberger, and B. A. Stickler, Gas induced friction and diffusion of rigid rotors, Phys. Rev. E **97**, 052112 (2018).

[43] J. Eismann, L. Nicholls, D. Roth, M. A. Alonso, P. Banzer, F. J. Rodríguez-Fortuño, A. V. Zayats, F. Nori, and K. Y. Bliokh, Transverse spinning of unpolarized light, Nat. Photonics **15**, 156 (2021).

[44] Y. Chen, F. Wang, Z. Dong, Y. Cai, A. Norrman, J. J. Gil, A. T. Friberg, and T. Setälä, Structure of transverse spin in focused random light, Phys. Rev. A **104**, 013516 (2021).

[45] J. J. Gil, A. T. Friberg, A. Norrman, and T. Setälä, Effect of polarimetric nonregularity on the spin of threedimensional polarization states, New. J. Phys. **23**, 063059 (2021).

[46] L. Novotny and B. Hecht, *Principles of Nano-Optics*, 2nd ed. (Cambridge University Press, Cambridge, England, 2012).

[47] B. Stickler, K. Hornberger, and M. Kim, Quantum rotations of nanoparticles, Nat. Rev. Phys. **3**, 589 (2021).

[48] J. J. Gil, Intrinsic Stokes parameters for 3D and 2D polarization states, J. Eur. Opt. Soc. **10**, 15054 (2015).

[49] C. P. Blakemore, A. D. Rider, S. Roy, Q. Wang, A. Kawasaki, and G. Gratta, Three-dimensional forcefield microscopy with optically levitated microspheres, Phys. Rev. A **99**, 023816 (2019).

[50] M. Guo, A. Norrman, A. T. Friberg, and T. Setälä, Probing coherence Stokes parameters of three-component light with nanoscatterers, Opt. Lett. **47**, 2566 (2022).